

# Simulation of the Shape of Micro Geometries generated with Jet Electrochemical Machining

M. Hackert<sup>\*1</sup>, G. Meichsner<sup>2</sup>, A. Schubert<sup>1,2</sup>

<sup>1</sup>Chemnitz University of Technology, Chair Micromanufacturing Technology

\*09107 Chemnitz, Germany, matthias.hackert@mb.tu-chemnitz.de

<sup>2</sup>Fraunhofer Institute for Machine Tools and Forming Technology

**Abstract:** Jet Electrochemical Machining (Jet-ECM) is an unconventional procedure for micromachining [1, 2, 3]. Based on localized anodic dissolution three-dimensional geometries and microstructured surfaces can be manufactured using Jet-ECM. The main advantage compared to other electrochemical procedures is, that the jet restricts the electric current density to a limited area. An air assistance developed at Chemnitz UT and Fraunhofer IWU allows to apply small working gaps of about 100  $\mu\text{m}$  [2]. Due to the high mean velocity in the jet of about 20 m/s the electrolyte supply is sufficient for using continuous direct current and higher dissolution rates compared to pulsed ECM are possible. In this study COMSOL Multiphysics is used to simulate the electric current density in the jet and the dissolution process in a time dependent model for Jet-ECM point processing, that means without a movement of the nozzle. Simulation and reality show a good coincidence.

**Keywords:** Jet Electrochemical Machining, localized anodic dissolution, mesh displacement, closed electrolytic free jet

## 1 Introduction

Electrochemical Machining with a closed electrolytic free jet is a special procedure to generate complex micro structures by help of anodic dissolution. The work piece shape is fabricated by supplying electrolytic current through an electrolyte jet ejected from a small nozzle. Only the work piece material exposed to the jet is removed because the current is restricted to the area limited by the jet like illustrated in figure 1. Supplying enough fresh electrolyte within the jet continuous direct current with mean current densities up to 1000 A/cm<sup>2</sup> can be ap-

plied. An additional jet of compressed air removes electrolyte directly after impinging on the work piece [2]. So working gaps between work piece and nozzle of down to 100  $\mu\text{m}$  can be used.

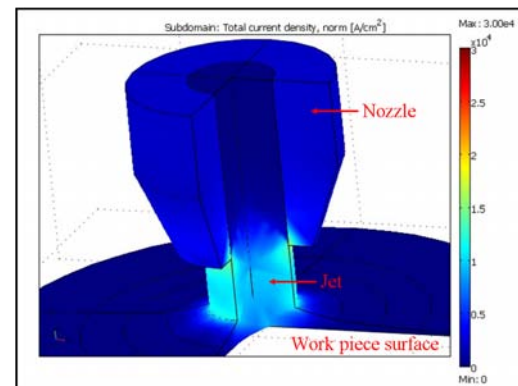


Figure 1: Stationary 3-D model of Jet-ECM current density

Complex three-dimensional micro geometries can be machined by moving the nozzle and controlling the electric current. Figure 2 shows as machining example three coaxial circles with a maximum depth of 300  $\mu\text{m}$  and a total machining time of 11 min. The webs have a minimum width of 1  $\mu\text{m}$ . Remarkable are the sharp edges, scarp flanks and the smooth surface within the cavity.

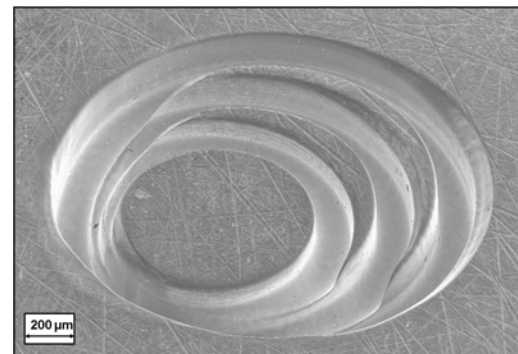


Figure 2: Example for Jet-ECM of stainless steel 1.4541

This work presents a pseudo-three-D model of a Jet-ECM point erosion process based on COMSOL Multiphysics. The model helps to understand and interpret experimental results which are made in stainless steel 1.4541.

## 2 Geometry and Mesh

Yoneda shows a rotational symmetric stationary model of Jet-ECM at time zero [4]. Based on this model the distribution of electric potential and current density are discussed in literature [3, 5]. From this work the geometries of nozzle, jet and work piece surface shown in figure 3 were derived. The nozzle has a diameter of 100  $\mu\text{m}$  and the working gap is 100  $\mu\text{m}$ , too. The work piece surface at time zero is the abscissa.

The FEM mesh at time  $t = 0\text{s}$  is shown in figure 4. The mesh consists of 3845 elements. It was generated using the automatic mesh creator with the option extra fine. In the origin of ordinates a maximum size of elements of 0,1  $\mu\text{m}$  was additionally defined because the area round these point will be most deformed due to the simulation of the dissolution process.

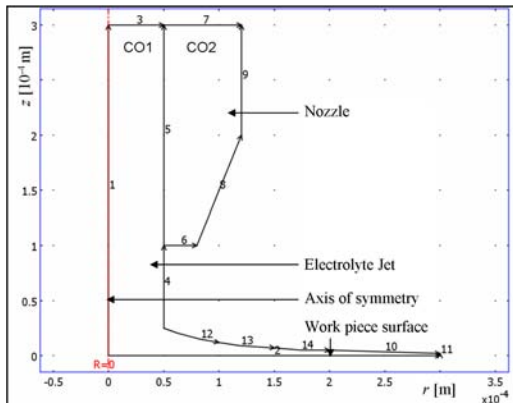


Figure 3: Geometry of the developed JET-ECM model

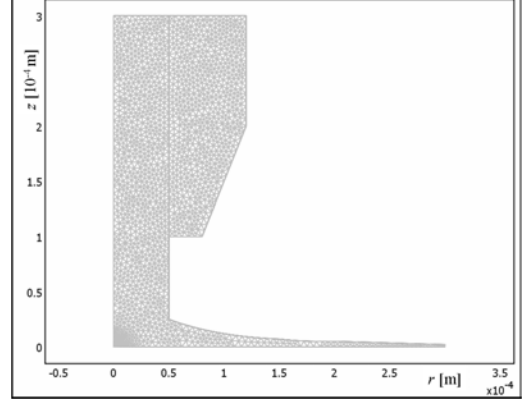


Figure 4: Mesh of the developed JET-ECM model

## 3 Electrodynamics

The application mode Conductive Media DC was used to define the electric parameters of the ECM process. In subdomain CO1, which represents the electrolyte, an isotropic electric conductivity was defined with the experimental value of 15,63 S/m. The material of the nozzle which can be located as subdomain CO2 in figure 3 was chosen out of the the COMSOL material library as steel AISI 4340 with a conductivity of  $4,032 \cdot 10^6$  S/m.

All electric boundary conditions are shown in table 1, where  $\varphi$  is the electric potential,  $\vec{n}_A$  is the normal vector and  $\vec{J}$  is the current density. The total voltage of 56 V over the working gap conforms the used power of the applied current supply, which has a maximum output of 1 A.

Boundary	Definition
1	axial symmetry
2	$\varphi = 56\text{ V}$
3	$\varphi = 0\text{ V}$
4	$\vec{n}_A \cdot \vec{J} = 0$
5	continuity
6	$\vec{n}_A \cdot \vec{J} = 0$
7	$\varphi = 0\text{ V}$
8-14	$\vec{n}_A \cdot \vec{J} = 0$

Table 1: Boundary conditions for the boundaries numbered in figure 3

## 4 Anodic Dissolution

The anodic dissolution which takes place on boundary number 2 is described as mesh displacement corresponding to Faradays' law with a velocity in normal direction  $\vec{v}_n$  depending to normal current density  $\vec{J}_n$  like shown in equation 1. The variables are shown in table 2.

$$\vec{v}_n = \eta \cdot \frac{M}{z_A \cdot \rho \cdot F} \cdot \vec{J}_n \quad (1)$$

Name	Value
$\eta$ current efficiency	
$M$ molar mass	55,06 g/mol
$z_A$ valency	3,436
$\rho$ mass density	7,76 g/cm <sup>3</sup>
$F$ Faraday const.	9,65·10 <sup>4</sup> C/mol

Table 2: Variables in equation 1 and used values for stainless steel 1.4541

The current efficiency  $\eta$  for Jet-ECM point processing of stainless steel 1.4541 was found out by help of micro weighing. The results of these investigations shows figure 5. From the deduced steady rise of  $m_{\text{eff}} = 165 \mu\text{g}/\text{C}$  the current efficiency is calculated in equation 2.

$$\eta = \frac{m_{\text{eff}} \cdot z_A \cdot F}{M} \approx 100 \% \quad (2)$$

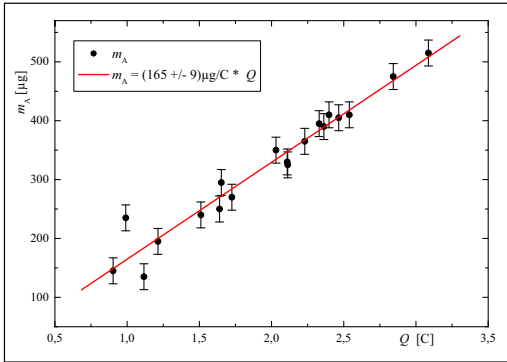


Figure 5: Mass removal as function of electric charge transfer for Jet-ECM point processing of stainless steel 1.4541

Because the current efficiency is not an efficiency like defined for energetic phenomena the value is not restricted to be lower than 100%. Even values larger than 100% can be found for electrochemical machining [6].

## 5 Results

The simulation and the experimental investigations were both made up to 2s processing time with a step size of 0,1s. An example result for the calculated deformation shows figure 6. The scale of displacement describes the last time step. The geometry shows the typical calotte shape of a Jet-ECM point processing like it's obvious in figure 7 for the same time step.

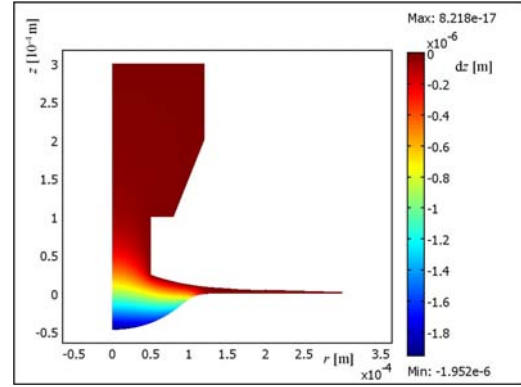


Figure 6: Surface plot of z-displacement at  $t = 0,5 \text{ s}$

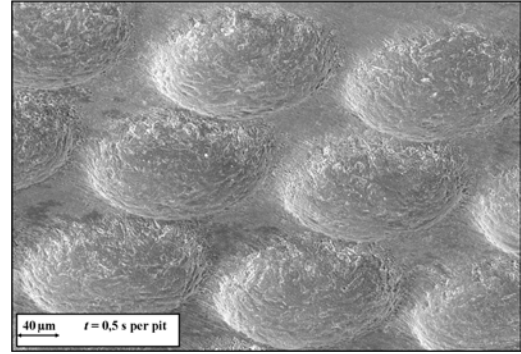


Figure 7: SEM image of an array of calottes generated with Jet-ECM point processing

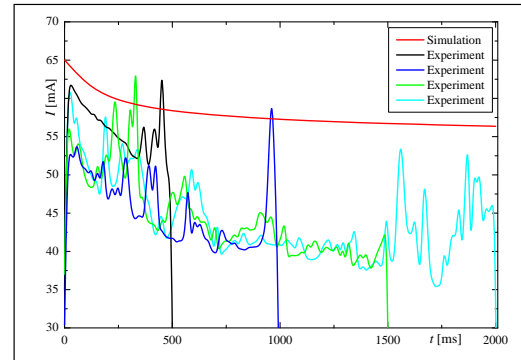


Figure 8: Total electric current as function of time for Jet-ECM point processing

Using boundary integration the simulated total electric current  $I$  was calculated. Figure 8 compares the calculated regime of  $I$  with four measured signals at different processing times. The model conforms very well the experimental current signals, especially below 500 ms time. Not at least the simulated currents are systematical about 10%-20% higher than the real current signals.

The shapes of machined calottes were measured with tactile profiling. Figure 9 compares simulated and generated profiles at four selected time steps. Up to 1 s processing time model and reality show a very good coincidence. With increasing processing time the experimental calottes are getting smaller and deeper than the calculated profiles.

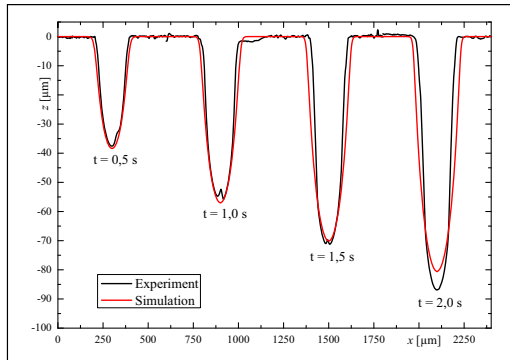


Figure 9: Comparison of simulated and generated Jet-ECM point erosions

## 6 Conclusions

In this study a model for a Jet-ECM point processing is presented, which is able to describe experimental results very well. In the model only electrodynamics and mesh displacement are used. It seems that due to the very good electrolyte supply in the closed electrolytic free jet and the localization of the current density within it, Jet-ECM can more easily be simulated than other applications of anodic dissolution [7].

The geometry of the model, especially the shape of the jet which was adopted from Yoneda [4] is usefully to calculate Jet-ECM point erosion up to about 1 s processing time.

Further steps will be simulations with different shapes for the area of the jet. Not at least the real profile of the impinging closed electrolytic free jet should be found out.

## References

- [1] M. Hackert, G. Meichsner, A. Schubert. Fast Micro Structuring with Electrolyte Jet Machining. *In: Proceedings of Fourth International Symposium on Electrochemical Machining Technology*, 1:123–128, 2007. ISBN 978-3-00-022770-7.
- [2] M. Hackert, G. Meichsner, A. Schubert. Generating Micro Geometries with Air assisted Jet Electrochemical Machining. *In: Proceedings of the euspen 10th Anniversary International Conference*, 2:420–424, 2008. ISBN 978-0-9553082-5-3.
- [3] W. Natsu, T. Ikeda, M. Kunieda. Generating complicated surface with electrolyte jet machining. *Precision Engineering*, 31:33–39, 2007.
- [4] K. Yoneda, M. Kunieda. A Numerical analysis of cross sectional shape of micro-indenters formed by the electrochemical jet machining. *J JSEME*, 29(62):498–516, 1996.
- [5] M. Kunieda, R. Katoh, Y. Mori. Rapid Prototyping by Selective Electrodeposition Using Electrolyte Jet. *CIRP Annals - Manufacturing Technology*, 47(1):161–164, 1998.
- [6] T. Haisch, E. Mittemeijer, J.W. Schultze. Electrochemical machining of the steel 100Cr6 in aqueous NaCl and NaNO<sub>3</sub> solutions: microstructure of surface films formed by carbides. *Electrochimica Acta*, 47:235–241, 2001.
- [7] R.V. Tijum. Electrochemical Machining in Appliance Manufacturing. *COMSOL NEWS*, 1:12–13, 2008.